BER the international journal of bridge engineering management and research

Use of Machine Learning in Bridge Inspection and Management in Ohio

AKM Anwarul Islam[1,*] and Natalie Rose[2]

Submitted: 06 February 2026 **Accepted:** 24 June 2026 **Publication date:** 10 July 2026

DOI: 10.70465/ber.v3i3.80

Abstract: As of 2022, the United States had 620,669 bridges that required regular inspections to ensure their safety and serviceability. These inspections are conducted in accordance with Federal Highway Administration regulations and are scheduled based on bridge condition and mandated inspection intervals. During each inspection, more than 100 bridge characteristics, including location, material, geometric, and operational data, are collected and used to determine the Structural Evaluation Rating (SER), a key indicator of overall bridge condition. This study investigates the application of machine learning techniques, including Pearson's correlation, decision trees, and random forest models, to identify and visualize relationships between bridge characteristics and the SER. The proposed methods are expected to provide rapid and reliable predictions of bridge condition based on selected characteristics and historical inspection data. In addition to improving prediction accuracy, these models offer intuitive visual interpretations of the factors influencing bridge performance. When integrated with existing inspection scheduling practices, these techniques may support more efficient and data-driven bridge management and may also assist engineers in selecting design characteristics that enhance long-term bridge performance.

Author keywords: Bridge management; machine learning; Pearson's correlations; decision trees; supervised and unsupervised models

Background and Literature Review

The objective of this research is to develop and apply machine learning techniques to improve and optimize highway bridge inspection scheduling and management. The proposed methods identify relationships between bridge characteristics and inspection ratings, providing valuable insights for more effective bridge management. In addition, these methods offer an intuitive and visual representation of the factors influencing bridge condition ratings.

Although many bridge engineering principles have remained unchanged for decades, bridge inspection practices continue to evolve with advances in technology. Modern inspection technologies enable engineers to collect and process significantly larger volumes of data than ever before. However, managing and analyzing this increased amount of information can be time-consuming and challenging. The integration of machine learning techniques can help engineers and inspectors make more informed decisions, improve inspection efficiency, and better prioritize bridges for maintenance, repair, and rehabilitation.

Machine learning is a branch of artificial intelligence that uses statistical models and algorithms to identify patterns within datasets and uncover underlying relationships among variables. In this study, several machine learning methods were employed to examine the relationships between bridge characteristics and the Structural Evaluation Rating (SER). The SER is an overall bridge condition rating that ranges from 0 to 9 and is determined using the minimum value of the appraisal ratings. Bridges are classified according to their SER as follows: an SER $\geq$7 indicates a "Good" condition, an SER of 5–6 indicates a "Fair" condition, and an SER $\leq$4 indicates a "Poor" condition. Detailed descriptions of these classifications are provided in Table 1. The SER, together with key bridge characteristics, serves as a fundamental basis for bridge condition assessment and bridge management decision-making.

The methods investigated include Pearson's correlation (PC), K-means clustering, principal component analysis (PCA), decision tree (DT) modeling, and random forest (RF) modeling. These techniques were selected because of their ability to efficiently process and analyze large datasets. The visual representations generated by these methods help improve the interpretation of relationships among variables, supporting bridge ranking and prioritization efforts. They also provide structured workflows that can be applied to the evaluation of individual bridges. Alternative methods

*Corresponding Author: AKM Anwarul Islam.
Email: aaislam@ysu.edu
[1]Professor, Civil and Environmental Engineering, Youngstown State University, 1 Tressel Way, Youngstown, OH 44555
[2]Former Graduate Student, Civil and Environmental Engineering, Youngstown State University, Youngstown, OH 44555

Discussion period open till six months from the publication date. Please submit separate discussion for each individual paper. This paper is a part of the Vol. 3 of the International Journal of Bridge Engineering, Management and Research (© BER), ISSN 3065-0569.

Table 1. Item appraisal rating codes for SER

Code	Description
N	Not applicable
9	Superior to present desirable criteria
8	Equal to present desirable criteria
7	Better than present minimum criteria
6	Equal to present minimum criteria
5	Somewhat better than minimum adequacy to tolerate being left in place as is
4	Meets minimum tolerable limits to be left in place as is
3	Basically intolerable requiring high priority of corrective action
2	Basically intolerable requiring high priority of replacement
1	This value of rating code not used
0	Bridge closed

may require more extensive data preprocessing or greater computational resources.

Bridge inspection is a time-consuming process for engineers, inspectors, and motorists. By introducing new approaches to optimization and efficiency, transportation agencies and consulting firms can adopt methods that reduce computational errors and shorten the time bridges remain functionally obsolete. Identifying the characteristics that most strongly influence inspection ratings can also guide the design of future bridges to improve long-term performance. In addition, these relationships may be incorporated into new bridge rating systems or used to enhance existing evaluation programs.

In 2022, Ohio managed more than 27,000 bridges, the second-highest total among all U.S. states. Approximately 4.5% of Ohio's bridges were classified as poor, as shown in Fig. 1. The estimated cost to replace all poor-rated bridges exceeded $1 billion, while the estimated cost to rehabilitate them was more than $700 million.[1]

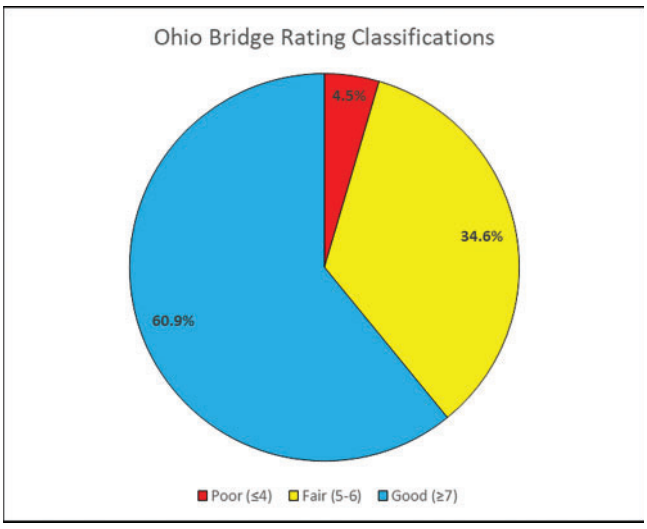

Figure 1. Structural evaluation rating classifications for all Ohio bridges

The Federal Highway Administration (FHWA) requires all states to comply with the National Bridge Inspection Standards (NBIS), which were first implemented in 1971.[2] These standards were established in response to the catastrophic collapse of the Silver Bridge over the Ohio River on December 15, 1967. The NBIS regulations define inspection procedures, inspector qualifications, and requirements for bridge inventories, reports, and condition ratings for all bridges within the public transportation network. This information is compiled in the National Bridge Inventory (NBI), a publicly accessible database containing annual bridge data for each state since 1992. The NBI supports public safety and enables transportation agencies to make informed decisions regarding the maintenance, preservation, and funding of the nation's transportation infrastructure.

Routine bridge inspections are conducted at intervals not exceeding 24 months, with approximately 83% of the nation's bridges inspected on this schedule.[3] State Departments of Transportation (DOTs) may require more frequent inspections than the federal minimum. Additional inspections may also be necessary when a bridge exhibits unexpected deterioration, damage, or other structural concerns. Inspections are performed visually and physically by teams of at least two inspectors. Bridges are accessed using snooper or bucket trucks, rappelling and climbing techniques, wading, or other terrain-navigation methods. Inspectors use hand tools, including scrapers, brushes, probing rods, and borers, to identify and measure defects. Bridge conditions and observations are documented on inspection forms and supported with photographic records. The Ohio Department of Transportation (ODOT) currently utilizes 14 inspection types with varying inspection frequencies, as summarized in Table 2.[4]

Since 2021, these inspection frequencies have outlined ODOT's prioritization using reliability-based inspection intervals.[4] This is performed using a bridge program called AssetWise, which tracks high-risk bridges by considering the following five critical features of a bridge.

Table 2. Ohio bridge inspection types and frequency

Inspection type	Frequency
Initial	Infrequent, performed and inventoried before the bridge is first opened to traffic or there is a change or update in inspection responsibility.
Routine	Performed at a maximum interval of 24 months based on reliability criteria.
In-depth	As-needed, generally for major or complex bridges often on a 60-month cycle or less.
Damage	As-needed.
Flood	As-needed.
Fracture critical	Not to exceed 24-months for structures that fit the rigid definition.
Underwater	Not to exceed 60-months.
Cross channel profile	As-needed.
Scour susceptibility inspection and evaluation	As-needed.
Special/interim	As-needed.
Safety (cursory)	
Quality assurance	A rolling sample set of field and office visits performed regularly by FHWA, ODOT Central Office, CEAO or initiated by any Control Authority or NBIS Program Manager to verify quality inspections.
Complex	Routine, with often a 60-month in-depth inspection cycle.

Note: CEAO—County Engineers Association of Ohio.

i. The presence of at least one fracture-critical member (FCM), which may occur in steel bridges and can result in a total loss of structural integrity if damaged.
ii. The susceptibility to scour, which occurs when water erodes or degrades streambeds beneath piers and abutments. Scour holes can occur more suddenly than other types of bridge deterioration and can affect the integrity and stability of the entire structure.
iii. The presence of a posted load or restriction on the bridge. Posted loads or restrictions are used when the capacity of the structure to carry its design or current legal load is reduced.
iv. The general appraisal or deck condition rating is less than seven.
v. If the bridge is a new construction or has had rehabilitation in the past three years. New construction or rehabilitation inspections are necessary to confirm that the design plans and requirements have all been met by the contractors.

Any defects or issues identified during these inspections can be addressed before the bridge is opened or reopened to traffic. This helps protect public safety while minimizing traffic disruptions and reducing delays caused by extended closures or detours. When any of these five critical features are identified during an inspection, AssetWise automatically adjusts the inspection interval. This adjustment increases the inspection frequency from the standard 24-month interval to a 12-month interval. Bridges that do not exhibit any of these critical features remain on the standard 24-month inspection schedule unless a non-routine inspection is warranted.

Bridge Inspection Technologies

Analysis of bridge condition ratings in Ohio indicates that the average SER for steel and concrete bridges increased by nearly one point in 30 years between 1992 and 2022, as shown in Fig. 2. However, this improvement should be interpreted with caution, as the construction of new bridges and the removal of poorly rated bridges may positively influence the statewide average. Several factors have likely contributed to this trend, including advances in design methodologies, construction practices, inspection technologies, rehabilitation techniques, material performance, and bridge replacement programs. Improved design approaches developed through research and lessons learned from structural failures have enhanced bridge safety and performance. For example, deficiencies in gusset plate design were identified as a contributing factor in the collapse of the I–35 W Bridge in 2007. Advances in materials and manufacturing processes have also improved durability, strength, and service life. In addition, emerging inspection technologies, such as ground-penetrating radar and ultrasonic surface wave testing, allow inspectors to evaluate internal conditions with minimal damage, cost, and disruption.[5]

Bridge deterioration results from a variety of factors, including accidental damage, material degradation, and environmental exposure. Unexpected events often require immediate attention to preserve structural integrity and public safety. In 2021, more than 13,000 vehicle–bridge collisions were reported in the United States.[6] Such impacts can damage columns, piers, girders, and other critical structural components, sometimes requiring bridge closure.

Environmental conditions also significantly influence bridge deterioration. While some effects, such as pavement

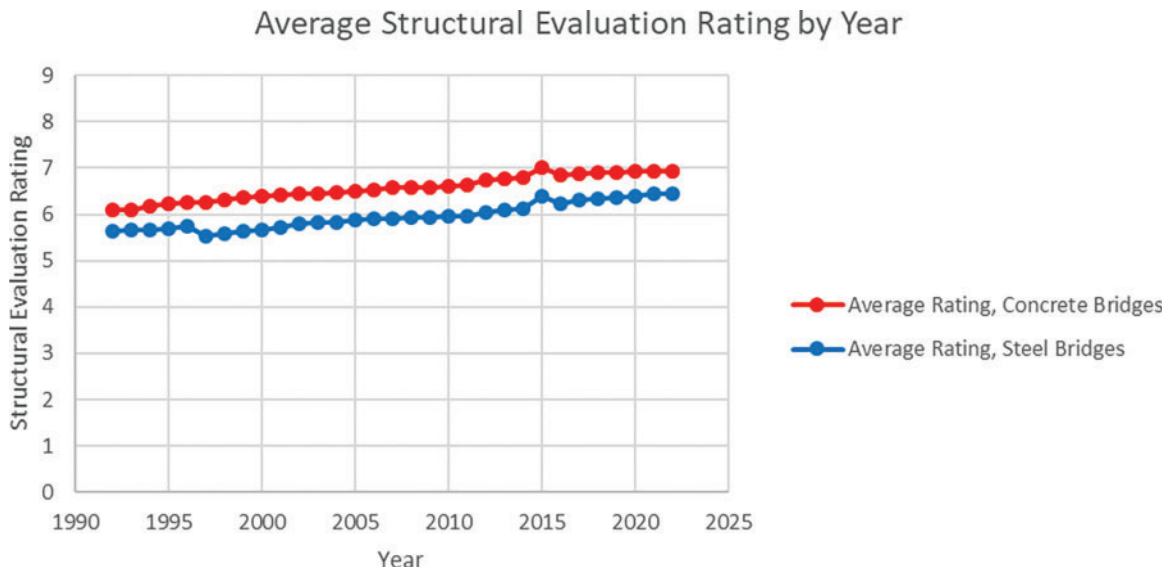

Figure 2. Average structure evaluation rating for Ohio bridges by year

potholes caused by seasonal weather changes, are easily observed, many forms of deterioration require detailed inspection to identify. Palu and Mahmoud[7] suggested that bridges in regions experiencing larger temperature fluctuations may face increased expansion-joint malfunctions as climate conditions evolve. In colder climates, repeated freeze-thaw cycles and the use of deicing salts can accelerate deterioration of concrete bridge decks and superstructures. Zhao et al.[8] found that concrete subjected to freeze-thaw damage experienced more severe deterioration when exposed to salt solutions similar to those used for winter maintenance. Bridge substructures located in waterways are particularly susceptible to scour and erosion caused by flowing water.

Technological advancements continue to improve the efficiency and accuracy of bridge inspections. Clarke-Sather et al.[9] identified report preparation and data compilation as among the most time-consuming aspects of the inspection process. Collecting and analyzing bridge data directly in the field can significantly reduce post-inspection processing time. Emerging technologies that integrate automation and machine learning may further streamline data management and decision-making. Abdallah et al.[10] provided a comprehensive review of current inspection technologies and proposed future frameworks for bridge assessment. One of the primary challenges identified was computational complexity. Machine learning methods that are both effective and interpretable can help address this challenge by enabling inspectors to implement advanced analytical tools with minimal training.

Recent research has also demonstrated the potential of robotic and remote inspection systems. Galdelli et al.[11] developed a robotic visual inspection platform equipped with multiple cameras capable of capturing high-quality images under a wide range of conditions. The system improved defect detection in areas that are difficult or hazardous for inspectors to access while reducing inspection time and cost. The authors also suggested that the data collected by such systems could support future machine-learning applications. Similarly, unmanned aerial vehicles (UAVs) have emerged as valuable tools for bridge inspections. UAVs can access areas that are difficult to reach using conventional methods, such as snooper trucks or rope access. Duque et al.[12] compared UAV-based damage assessments with traditional field measurements and found promising results. However, image quality remained sensitive to adverse weather and lighting conditions. Further research on the cost-effectiveness and reliability of UAVs under varying conditions could expand their role in bridge inspection programs.

Various machine learning methods have demonstrated significant value across a wide range of disciplines. In manufacturing, these methods are used to detect defects and optimize production processes. Altmann et al.[13] investigated supervised and unsupervised machine-learning techniques for defect classification in metal additive manufacturing. Using 635 processed micrographs, the researchers applied K-means clustering and RF models to identify and classify manufacturing defects. Among the methods evaluated, RF achieved the highest performance, exceeding 90% classification accuracy for all defect categories. In cybersecurity, machine learning has improved biometric authentication and network protection systems. Patro et al.[14] demonstrated that feature optimization techniques applied to electrocardiogram-based biometric data significantly improved recognition accuracy compared with existing classification approaches.

Armin and Hazem[15] used multi-target machine learning algorithms to simultaneously predict the condition of two core elements of the bridge, namely the deck and substructure. They used eXtreme Gradient Boosting (XGBoost) and RF models. For feature selection, the RF algorithm performed best on the training set, while the XGBoost performed best on the test set. For condition prediction, the

XGBoost achieved the highest accuracy on both the training and test sets.

Within bridge engineering, machine learning offers a practical, low-cost, and minimally invasive approach to structural health monitoring and damage detection. Luo et al.[16] reviewed computer-vision techniques for defect identification, vibration measurement, and parameter estimation. Li and Burgueño[17] evaluated five soft-computing methods, including support vector machines and fuzzy neural networks, for predicting deterioration in bridge abutment walls. Their results demonstrated that multiple modeling approaches can provide reliable predictions, allowing practitioners to select the method most appropriate for a specific application.

Ultimately, the most effective strategy for preserving the nation's bridge infrastructure is prevention. Early detection of defects provides agencies with greater flexibility and resources to implement corrective actions before conditions worsen. Routine inspections remain the cornerstone of this preventive approach. Advances in sensors, UAVs, robotic systems, and other inspection technologies have expanded engineers' ability to assess bridge components that were previously difficult to access or evaluate. The integration of machine learning into bridge inspection, health monitoring, and asset management represents another important advancement. The methods presented in this research offer practical and interpretable tools that have the potential to improve bridge management and contribute to the next generation of infrastructure assessment technologies.

Data Preprocessing

In this research, the term "bridge" is defined in accordance with FHWA guidelines as "a structure of more than 6.1 meters (20 ft) in length spanning an obstruction or depression".[18] The bridge data used in this study were obtained from the NBI repository, which provides annual inspection records for highway bridges throughout the United States and its territories. For each inspection year, the repository offers three data-access options: individual files for each of the 54 states and territories, a single file containing all bridges from all states and territories, and a file containing all records for that year. Each state is responsible for inspecting its public highway bridges and maintaining compliance with the NBIS. While all states must satisfy the minimum federal requirements, individual DOTs may adopt additional inspection procedures and regulations that are more stringent than those required by the FHWA.

This study focuses exclusively on bridges located in Ohio. Restricting the analysis to a single state provides greater consistency in inspection practices, reporting procedures, and regulatory requirements across all years of the dataset. Ohio was selected because it manages more than 27,000 bridges annually, providing a large and comprehensive dataset for analysis. Although all states follow FHWA inspection requirements, variations in state-specific regulations, inspection practices, climate conditions, population density, and infrastructure characteristics can introduce additional sources of variability. Limiting the study to Ohio reduces these external influences and improves the consistency of the analysis.

After selecting the state and inspection years, the raw NBI data were downloaded as delimited files and imported into a Microsoft Excel workbook containing 31 worksheets, representing each year from 1992 through 2022. Each worksheet was assigned a unique identifier based on the state abbreviation and the last two digits of the inspection year (e.g., "OH22" for Ohio bridge data from 2022).

The raw dataset contains up to 134 variables, each representing a specific bridge characteristic. Depending on the year, the dataset includes between 26,986 and 28,284 bridge records. Over time, bridges are constructed, rehabilitated, closed, or demolished; therefore, some bridges appear throughout the entire 31-year period, while others are present only for a portion of the study duration. Across all years, the dataset contains as many as 856,986 bridge records. Each record corresponds to a single bridge and includes all associated characteristics collected during the inspection. Bridges are uniquely identified by their structure number (SN), a numeric identifier used solely for identification purposes. To ensure consistency and facilitate data management, each worksheet was sorted by SN prior to analysis.

Characteristic Information

The characteristic columns provided in the raw datasets contain geospatial, physical, historical, and geometric information. Over the 31-year study period, new characteristics were added to inspection records, while others were removed as technologies and data collection practices evolved. To ensure consistency across the dataset, only characteristics that were available throughout the entire 31-year period were retained. This approach enables meaningful comparisons using both the raw data and the results of this study over any time span within the dataset.

Historical information, such as federal land designation, is primarily used to identify bridges for administrative or organizational purposes. Geospatial information, including location and latitude, provides reference data for locating bridges within Geographic Information Systems and other mapping frameworks. Although location data may assist in identifying environmental or climatic conditions, these characteristics are descriptive rather than causal and do not directly contribute to bridge deterioration. Therefore, historical and geospatial variables were excluded from the analysis.

Bridge geometry is highly variable and is directly related to the materials, loads, and service conditions experienced by a structure. Geometric configurations depend on the type of obstacle being crossed, operational requirements, and owner preferences. While design standards establish minimum requirements, many geometric characteristics are determined by engineers and bridge owners. To focus on the variables most relevant to bridge performance and condition

while simplifying data processing, only eight key characteristics directly associated with bridge health and management were selected for analysis.

Bridges are commonly constructed from concrete or steel, materials with substantially different mechanical properties and responses to environmental conditions. To account for these differences, the "structure kind" variable was retained initially and used to separate the dataset into steel and concrete bridge groups. Once the data were divided, this variable was no longer needed and was removed from the final workbooks.

Age was calculated as the difference between the inspection year and the value in the "year built" column. "Year built" is recorded as a four-digit code representing the year the bridge was completed or the best available estimate. Similarly, "age reconstructed" was calculated as the difference between the inspection year and the value in the "year reconstructed" column. This field is also recorded as a four-digit year, with bridges that have not been reconstructed coded as 0000.

Reconstruction refers to work that qualifies for Federal-aid funding and meets established eligibility requirements. A bridge component is considered reconstructed when the work substantially alters the bridge's geometry or load-carrying capacity. Temporary repairs intended only to maintain serviceability until a permanent solution is implemented are not classified as reconstruction. For example, resurfacing a bridge deck is considered a repair, whereas replacing a deck while modifying lane configurations or adding sidewalks constitutes reconstruction. Both bridge age and age since reconstruction may reflect material deterioration, changes in structural properties, and the cumulative effects of long-term loading.

"Average daily traffic" (ADT) represents the most recent measured or estimated traffic volume on the inventory route. It is recorded as a six-digit value representing up to one million vehicles per day. ADT serves as an indicator of the daily traffic demand placed on a bridge. Higher traffic volumes can increase wear on bridge components, potentially accelerating deterioration and reducing service life.

"Percent ADT truck" is a two-digit value representing the percentage of truck traffic within the ADT volume. This category excludes vans, pickup trucks, and other light-duty vehicles and may be estimated based on roadway classification. Because trucks generate larger and more concentrated loads than passenger vehicles, the percentage of truck traffic is an important consideration in bridge design and maintenance. Accurate estimates help engineers account for heavier loading demands and reduce stress-related deterioration over the bridge's service life.

"Main unit spans" is the number of spans within the bridge's primary structural unit. This generally includes all spans for most bridges, the principal unit of a large structure, or a section constructed using a different material or design than the approach spans. The value is recorded as a three-digit number. Bridges with multiple main spans may incorporate varying span lengths, beam configurations, or design features, which can influence both inspection procedures and the types of deterioration experienced.

"Maximum span length" is the length of the longest span within the bridge, measured along the centerline in metric units. Measurements may be taken from center-to-center bearing points or as the clear distance between piers, bents, or abutments. This value is recorded as a five-digit number. Longer spans generally experience greater deflections under load than shorter spans subjected to similar loading conditions. As a result, monitoring span behavior is particularly important for superstructures containing FCMs.

"Structure length" is the total length of the bridge roadway, measured from paving notch to paving notch or from the backwall of one abutment to the backwall of the opposite abutment. It is recorded in metric units using a six-digit code and measured to the nearest tenth. Unlike maximum span length, structure length represents the bridge as a whole and is useful for evaluating how loads are distributed throughout the entire structure and its support system.

"Deck width" is the out-to-out width of the bridge deck, measured either as the lateral clearance between superstructure members or as the actual deck width, depending on the bridge configuration. It is recorded in metric units using a four-digit code and measured to the nearest tenth. Deck width is largely determined by the transportation needs of the area served by the bridge. Wider decks can distribute vehicular and pedestrian loads across a larger area, reducing load concentration compared to narrower structures.

The "structural evaluation" column contains the SER value, which is the target variable of this research. After removing all other variables, the Steel Bridge Data and Concrete Bridge Data workbooks were finalized and prepared for analysis. Fig. 3 presents a sample of the final Steel Bridge Data workbook.

Complete Data and Materials

Some bridges did not contain a complete set of information for all characteristics. In some cases, a characteristic was not applicable to an individual bridge and was coded with an "N." To prevent the program from processing inapplicable information, any row containing an "N" was discarded. In other cases, no information was recorded for a characteristic. This was especially prevalent in earlier inspection years. This lack of information may have occurred because the bridge did not exhibit the characteristic, or the bridge element was not accessible during inspection, or because of inspector error. For ease of data processing, any rows containing blank cells were also discarded. This process was repeated for all 31 years of data. As a result, the remaining dataset included only bridges with complete sets of information, as shown in the example in Fig. 3.

After retaining only complete datasets, four copies of the consolidated workbook were created to allow comparisons between different bridge materials. The structure kind column identifies bridge material by code. Table 3 shows the bridge material classifications and their corresponding code numbers from this column.[18]

The first workbook (Concrete Bridge Data) contains bridges utilizing concrete, concrete continuous, prestressed

STRUCTURE_NUMBER	AGE	ADT	MAIN_UNIT_SPANS	MAX_SPAN_LEN	STRUCTURE_LENGTH	DECK_WIDTH	STRUCTURAL_EVAL	YEAR_RECONSTRUCTED	PERCENT_ADT_TRUCK
0100021	39	4627	3	21.9	58.3	12.8	6	0	13
0100048	39	4627	3	21.9	59.1	12.8	6	0	13
0100137	44	3881	3	28.7	73.8	12.2	6	0	19
0100145	44	3881	3	28.7	73.9	12.2	7	0	19
0100226	44	3881	3	38.4	97.7	12.3	7	0	19
0100234	44	3881	3	38.4	97.5	12.2	7	0	19
0100331	50	2888	3	16.5	44.2	12.8	7	0	20
0100366	50	2888	3	16.5	44.4	12.8	6	0	20
0100420	50	2888	3	22.9	61.4	12.2	8	0	20
0100455	50	2888	3	22.9	61.6	12.2	8	0	20
0101397	23	3612	3	40	105.1	14.1	7	0	8
0101842	24	3294	3	24.4	55.9	14.3	7	0	10
0101869	92	1108	3	30.8	77.8	12.2	5	1983	13

Figure 3. Final steel bridge data sample

Table 3. Main structure material and/or design based on NBI coding guide

Code	Name
1	Concrete
2	Concrete continuous
3	Steel
4	Steel continuous
5	Prestressed or Post-tensioned concrete
6	Prestressed or Post-tensioned concrete continuous
7	Wood or Timber
8	Masonry
9	Aluminum, Wrought Iron, or Cast Iron
0	Other

and post-tensioned concrete, and prestressed and post-tensioned concrete continuous spans. The second workbook (Steel Bridge Data) contained bridges with steel as the building material; these include steel and steel continuous spans. The third workbook (Steel and Concrete Bridge Data) contained both the steel and concrete spans together. The fourth workbook (Other Materials) contained bridges utilizing any other structural material, including wood or timber, aluminum, wrought iron, cast iron, or other spans. Steel and concrete bridges make up most of the remaining bridges, especially those located on the highway network. The third and fourth workbooks contain a small number of bridges and, therefore, were not considered for this analysis.

The Concrete Bridge Data and Steel Bridge Data workbooks are used for further analysis due to the ease of their year-to-year capabilities within the program. To run the DT and random forest (RF) models, copies of the workbooks were created and adjusted. In these copies, the data from each year was consolidated onto one sheet instead of 31 separate years. This was repeated to have one sheet of data for all 31 years, the last five years, and 2022 only. This was done for both concrete and steel bridge data. In total, six workbooks were created and used in this research. Table 4 provides the titles and descriptions of each workbook, while Table 5 indicates the final number of bridges considered for analysis within each data set per year.

Data Analysis and Modeling

The objective of this analysis is to determine the SER based on its relationship with selected bridge characteristics. Identifying the characteristics most strongly associated with deterioration may help prioritize bridges for more frequent inspections. Supervised machine learning models predict an output from labeled input data by learning patterns during training and are commonly used for regression and classification tasks. In contrast, unsupervised machine learning models analyze unlabeled data to identify underlying patterns, relationships, and structures through techniques, such as clustering, association analysis, and PCA. Both approaches were evaluated in this research for their pattern-recognition capabilities.

PC

PC measures the strength and direction of the linear relationship between two variables. The variables are plotted against each other, and a best-fit line is generated from the data points. The correlation coefficient, r, quantifies how closely the data points align with this line. Values of r range from −1 to 1. Negative values indicate an inverse relationship, while positive values indicate a direct relationship. A coefficient of zero indicates no linear relationship. Table 6 summarizes the ranges of r and their corresponding associations.

PC uses covariances and standard deviations to determine the relationship coefficient of two selected variables. The covariance (Covx,y) is a measure of variability between two

Table 4. Microsoft excel workbook summary

Excel workbook title	Bridge data included
2022 Concrete bridge data	Concrete bridges in 2022 only
2018–2022 Concrete bridge data	Concrete bridges from the last five years
1992–2022 Concrete bridge data	Concrete bridges for all years beginning in 1992
2022 Steel data bridge	Steel bridges in 2022 only
2018–2022 Steel data bridge	Steel bridges from the last five years
1992–2022 Steel bridge data	Steel bridges for all years beginning in 1992

Table 5. Final number of Ohio bridges considered every year

Year	Concrete bridges	Steel bridges
1992	7,829	10,746
1993	7,834	10,684
1994	8,135	10,590
1995	8,464	10,515
1996	8,567	10,404
1997	10,520	14,261
1998	10,750	14,099
1999	10,900	13,954
2000	11,271	13,810
2001	11,452	13,694
2002	11,682	13,381
2003	11,752	13,318
2004	11,873	13,194
2005	12,160	12,984
2006	12,287	12,816
2007	12,553	12,666
2008	12,770	12,553
2009	13,006	12,393
2010	13,087	12,241
2011	12,895	11,892
2012	12,857	11,707
2013	13,045	11,519
2014	13,170	11,398
2015	13,303	11,293
2016	14,118	11,432
2017	13,635	11,086
2018	13,711	10,977
2019	13,731	10,883
2020	13,719	10,798
2021	13,575	10,455
2022	13,621	10,383
Total	368,272	372,126

Table 6. Pearson's correlation coefficients association

Correlation coefficient (r)	Association
±1.0	Perfect positive or negative association
± 0.8 to 1.0	Strong positive or negative association
± 0.4 to 0.8	Moderate positive or negative association
± 0 to 0.4	Weak positive or negative association
0	No correlation

random variables and is calculated using Eq. (1).

$$Cov_{x,y} = \frac{\sum(x_i - \overline{x})(y_i - \overline{y})}{N - 1} \tag{1}$$

The standard deviation ($\sigma_{x,y}$) measures the dispersion of a dataset compared to the mean, calculated as the square root of the variance, as shown in Eq. (2).

$$\sigma_{x,y} = \sqrt{\frac{\sum(x_i - \mu)^2}{N}} \tag{2}$$

With this information, PC coefficient (r) can be determined using a ratio of the covariance and the product of the standard deviations, which is shown in Eq. (3).

$$r = \frac{Cov_{x,y}}{\sigma_x \sigma_y} \tag{3}$$

PC coefficients are calculated for each selected characteristic. Although these coefficients are produced in a tabular format, a heatmap can also be generated to provide an easily interpretable visual graphic. Coefficients and heatmaps were produced for each year from 1992 to 2022 for both steel and concrete bridges.

DT modeling

A DT is a supervised, non-parametric learning algorithm that classifies data and makes predictions using training subsets. It provides an interpretable, tree-structured model

in which rule-based branches guide data through decision nodes to possible outcomes while preserving key data characteristics.

The SER value is the target variable predicted using classes defined by the eight selected features. A random state is applied to ensure consistent data splitting across executions. The dataset is divided into training and test sets, with 80% used for training and 20% for testing and validation.

The DT algorithm is fitted to the training data. A fixed random state controls the estimator's random behavior during splitting, ensuring the tree structure remains consistent across runs. The trained model is then applied to the test set to predict SER values. Model performance is evaluated by comparing predicted and actual values.

The explained variance (r^2), or coefficient of determination, measures the proportion of variance in the dependent variable explained by the independent variables. It is calculated using the total sum of squares (TSS), which represents total variance, and the residual sum of squares (RSS), which represents unexplained variance after model fitting. The explained variance (r^2) is defined by Eq. (4):

$$r^2 = 1 - \frac{RSS}{TSS}. \tag{4}$$

The explained variance ranges from 0 to 1, with higher values indicating a better model fit.

The sum of squared errors (SSE) measures the discrepancy between actual (y) and predicted ($\hat{y}$) values. It is calculated as the sum of squared differences between them, with lower values indicating better performance. If predictions perfectly match observations, SSE equals zero. SSE is calculated using Eq. (5):

$$SSE = \sum (y - \hat{y})^2 \tag{5}$$

A DT is built branch by branch as rules are generated from the data. Each observation follows the applicable branches until it reaches a leaf node, which represents its final classification. The predicted SER is then compared with the actual value. A coefficient of determination is also calculated for each leaf to assess prediction accuracy within that node.

RF modeling

RF modeling is a supervised learning algorithm that improves prediction accuracy by combining multiple DTs. Rather than relying on a single tree, the model aggregates predictions from many independently trained trees, reducing overfitting and improving generalization. Each tree is built using a randomly selected subset of the data through a bagging process.

The RF models use the same dataset and Python libraries as the DT models. SER is the target variable, while the remaining features serve as predictors. A fixed random state ensures consistent data splitting and reproducible results.

An RF classifier containing 100 trees is trained and evaluated using classification accuracy. An RF regressor with 100 trees predicts SER values and is assessed using the R^2 score. Combined tree outputs produce a single generalized prediction.

Selection of Analysis Methods

Three analytical methods were selected to evaluate relationships between SER and the chosen characteristics: PC, DT, and RF modeling. Although DT and RF models operate under similar principles, they differ in how training data are processed. Applying both methods enables comparison of their strengths and limitations for predicting bridge health and supporting management decisions.

Other techniques, including K-means clustering and PCA, were considered but not used. These methods offer limited advantages when working with categorical data because measuring distances between categories is difficult. While the characteristics analyzed in this study are discrete or continuous, future bridge inspection data may include categorical or ordinal variables. To maintain flexibility for analyzing a broader range of characteristics, methods better suited to mixed data types were selected. Table 7 summarizes the analytical methods used.

Results and Discussions

Both steel and reinforced concrete bridges undergo deterioration from fatigue, freeze-thaw cycles, corrosion, vehicular loads, and other environmental distresses. However, the

Table 7. Summary of supervised and unsupervised learning methods

Learning method	Method type	Summary
K-means clustering	Unsupervised	Clusters data based on similar features
Principal component analysis	Unsupervised	Transforms data into lower dimensional forms
Pearson's correlation	Statistical	Measures linear correlation between two sets of data
Decision tree modeling	Supervised	Categorizes data based on training information to make predictions
Random forest modeling	Supervised	Categorizes data based on multiple randomized training information to make predictions

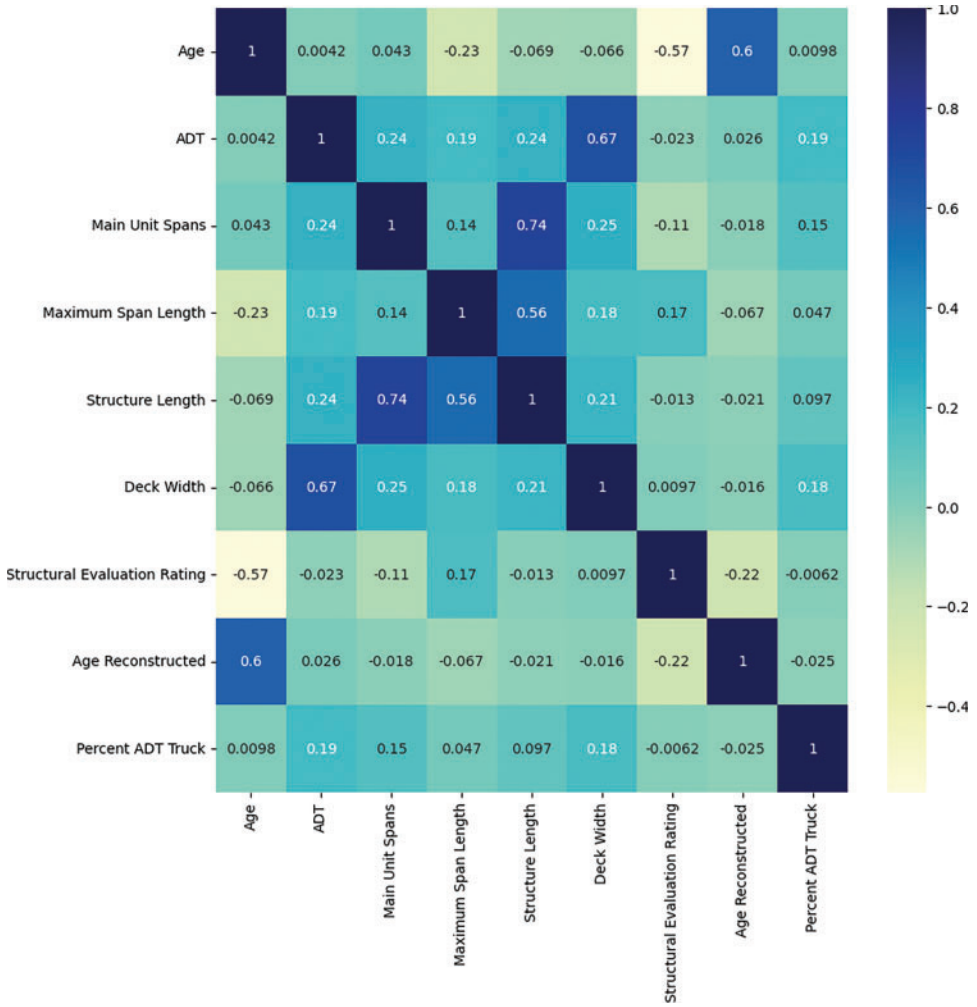

Figure 4. Pearson's correlation heatmap for 2022 concrete bridge data

average SER has been increasing instead of decreasing in both bridge types over time. This can be attributed to more efficient and precise design methods, better inspection tools and techniques, and preventative maintenance. The SER may also be dependent on the inspectors, with 95% of condition ratings varying by two points and 68% varying within one point for each element.[19] Utilizing machine learning becomes valuable for predicting the SER by removing inspector bias and only considering the raw data.

PC results

PC coefficients were calculated for each characteristic annually. Fig. 4 presents the correlation matrix for the 2022 Concrete Bridge dataset. The heatmap uses colors and numerical values to visualize the strength and direction of correlations between characteristics. A characteristic correlated with itself has a coefficient of 1, indicating a perfect relationship, while a coefficient of 0 indicates no relationship.

Although the matrix displays relationships among all characteristics, this study focuses only on correlations with SER. Correlation matrices provide a clear and interpretable way to examine relationships within each year, offering greater visual insight than tabulated results alone. Heatmaps were generated for both Concrete Bridge and Steel Bridge datasets from 1992 to 2022, resulting in 31 annual correlation matrices for each bridge type.

PC coefficients were calculated for all 31 years of data. To identify long-term trends, the average coefficient for each characteristic was determined across the entire study period. While these averages provide an overall measure of relationship strength, they may mask temporal changes in importance. Examining shorter periods, such as individual years or rolling five-year averages, can reveal shifts caused by evolving design practices, technologies, or maintenance strategies. Considering multiple timeframes provides complementary perspectives for decision-making and facilitates comparison between concrete and steel bridges.

Table 8 presents the average correlation coefficients for each characteristic, while Fig. 5 compares these values by bridge material. This comparison highlights characteristics with differing relationships to SER and provides a visual assessment of their relative importance. In six of the eight characteristics, the correlation sign was consistent across both materials. However, ADT and main unit spans showed negative correlations for concrete bridges and positive correlations for steel bridges. Such differences may result from

Table 8. Characteristics average 31-year Pearson's correlation coefficient by material

	Average correlation	
Characteristic	Concrete bridges	Steel bridges
Age	−0.5806	−0.4594
ADT	−0.0433	0.1585
Main unit spans	−0.0772	0.1336
Maximum span length	0.2110	0.1384
Structure length	0.0202	0.1189
Deck width	0.0123	0.2847
Age reconstructed	−0.1871	−0.2163
Percent ADT truck	0.0096	0.1816

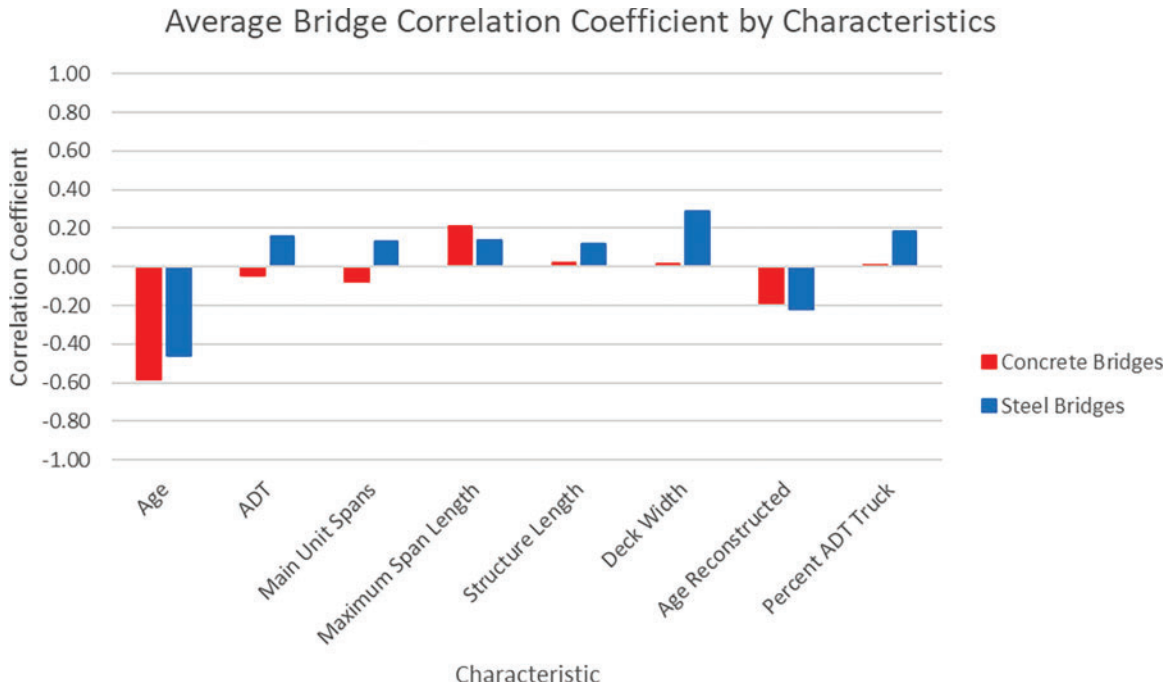

Figure 5. Average of 31-year Pearson's correlation coefficients based on the material of construction

unaccounted factors influencing bridge performance. Correlations near zero are also more likely to change sign than stronger positive or negative relationships because only small numerical shifts are required.

Averaging correlation coefficients across 31 years could produce unrepresentative results if coefficient signs changed over time. However, although these two characteristics exhibited weak relationships, their coefficient signs remained consistent throughout the study period. This indicates that the long-term averages accurately reflect their overall relationships and are not artifacts of temporal variation.

Figs. 6 and 7 illustrate annual fluctuations in correlation coefficients, making it easy to identify positive, negative, and near-zero relationships. These visualizations provide a clearer comparison of bridge materials and characteristics than tables alone. They also help reveal the effects of changes in specifications, inspection practices, environmental events, or data collection methods. For example, the introduction of new technologies may create trends in subsequent years. Analyzing specific time periods can further isolate such effects and support targeted engineering decisions.

Age and age reconstructed consistently showed negative correlations with SER for both bridge materials over 31 years. Age had the strongest, though only moderate, relationship with SER, while age reconstructed ranked third overall but remained weak. As bridges age, exposure to weather, chemicals, impacts, and repeated loading reduces conditions reflected in negative coefficients. Early inspections can identify deterioration, enabling component replacement or full reconstruction. LeBeau and Wadia-Fascetti[20] highlighted the importance of early inspection for detecting corrosion in strands and rebars. Prior work by Agrawal et al.[21] did not account for abrupt changes, such as rehabilitation or data

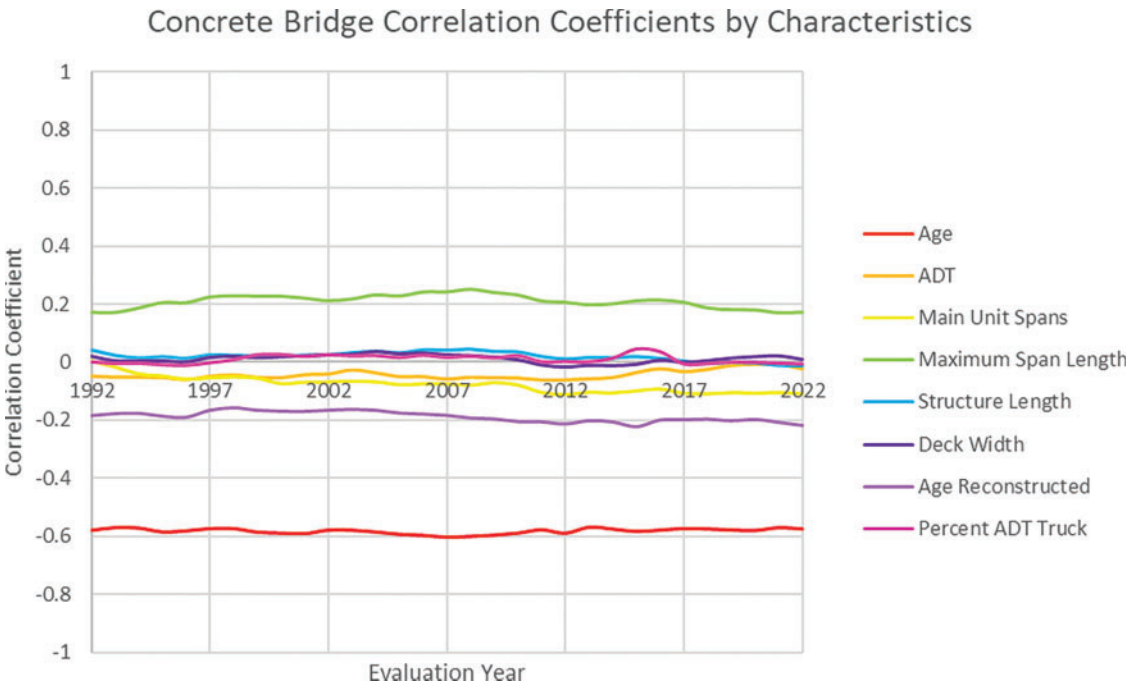

Figure 6. Pearson's correlation coefficients over time for concrete bridges

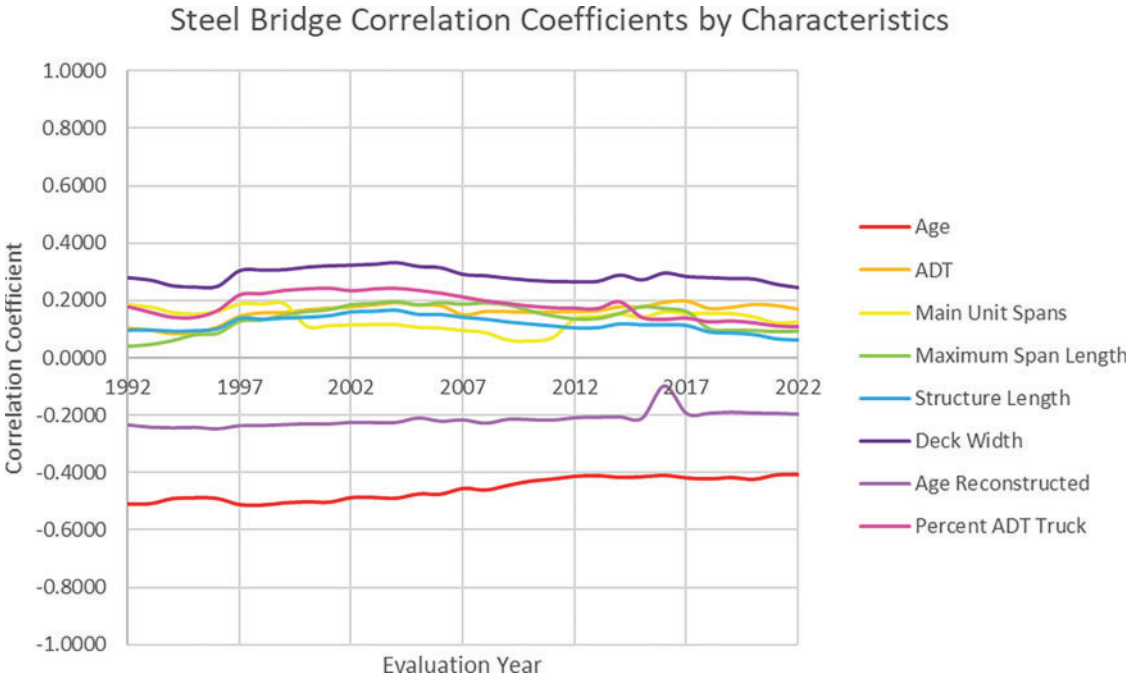

Figure 7. Pearson's correlation coefficients over time for steel bridges

errors. Reconstruction resets bridge age by replacing most components.

Except for age, all variables exhibited weak or negligible correlations with SER. Although these relationships were weak, they can still be ranked relative to one another. For both steel and concrete bridges, ADT showed the fifth-strongest correlation with SER. However, the correlation was positive for steel bridges and negative for concrete bridges. ADT reflects repeated traffic loading, which has been linked to increased bridge deterioration through more frequent load cycles, greater use of deicing agents, and fatigue damage.[22,23] Despite these effects, ADT demonstrated only weak or no correlation with SER in either bridge type.

The number of main unit spans exhibited the fourth-strongest relationship with SER for concrete bridges and the seventh-strongest for steel bridges. Maximum span length ranked second for concrete bridges and sixth for steel bridges. Although load distribution patterns may be similar between long and short spans on the same bridge, longer

spans carry greater total loads due to increased self-weight and vehicular loading. These loads result in larger midspan deflections and higher internal stresses, which could accelerate deterioration.

Structure length ranked sixth for concrete bridges and eighth for steel bridges. Because structure length only measures the distance between paving notches, it does not account for the number of supports, span configurations, or individual span lengths. Consequently, it may not accurately represent the forces, moments, and stresses experienced by the bridge. Longer bridges often require additional structural components, such as larger decks, more girders and piers, and greater superstructure anchorage. While these features may increase potential deterioration points, both concrete bridges and steel bridges exhibited only weak correlations between structure length and SER. This suggests that structure length alone is insufficient to explain SER variation and that its influence may depend on interactions with other characteristics.

Deck width ranked second for concrete bridges and seventh for steel bridges, yet both bridge types showed only weak positive correlations with SER. Bridge decks are directly exposed to traffic loads, weather, and deicing agents, making them particularly susceptible to deterioration. Deck width is largely determined by functional requirements, including the number of traffic lanes, shoulders, bicycle lanes, sidewalks, and safety barriers. These design elements vary according to traffic demand, site conditions, and owner requirements. Although wider decks may present more potential deterioration areas, they can also distribute loads more effectively. For example, bridges with wider shoulders or pedestrian facilities may experience lower live-load demands than bridges of equal width carrying only vehicular traffic. This may help explain the observed positive relationship between Deck width and SER.

Aside from age and age reconstructed, the ranking of bridge characteristics differed between concrete bridges and steel bridges. Many observed correlations were weaker or differed from expected trends, and the small differences between coefficient values make rankings sensitive to minor fluctuations. Overall, the analysis indicates that geometry alone has limited influence on SER. Nevertheless, PC analysis remains valuable for identifying trends, guiding further investigation, and highlighting age as the most influential factor affecting bridge condition and long-term performance. These findings underscore the importance of preventive maintenance and comprehensive inspection records in managing aging infrastructure effectively.

DT and RF model results

Using DT and RF modeling, it was possible to associate the selected characteristics with the correct SER reliably for both bridge types. Two timespans were processed: all recorded years from 1992 to 2022 and the last five recorded years from 2018 to 2022. The corresponding accuracy scores are shown in Table 9.

Model performance was similar for both Concrete Bridge and Steel Bridge datasets, with the largest difference in accuracy being 2.5% in the five-year DT model. This suggests that both DT and RF models can effectively predict SER regardless of bridge material, despite the datasets differing by approximately 4,000 bridges. Model performance was also consistent across timeframes. The largest accuracy difference between the 1992–2022 and 2018–2022 Concrete Bridge datasets was 2.9%, occurring in the DT model. Across all datasets, both model types achieved accuracies above 79%. The explained variances are presented in Table 10.

Explained variance ranges from 0 to 1, with values closer to 1 indicating a better model fit. The 31-year datasets produced the highest explained variances for both bridge

Table 9. Decision tree and random forest model accuracy percentage by material

		Concrete bridges	Steel bridges
1992–2022	Decision tree	82.1%	82.9%
	Random forest	87.9%	86.2%
2018–2022	Decision tree	79.2%	81.7%
	Random forest	88.0%	88.5%

Table 10. Decision tree and random forest model explained variances by material

		Concrete bridges	Steel bridges
1992–2022	Decision tree	0.786	0.809
	Random forest	0.877	0.881
2018–2022	Decision tree	0.705	0.740
	Random forest	0.838	0.861

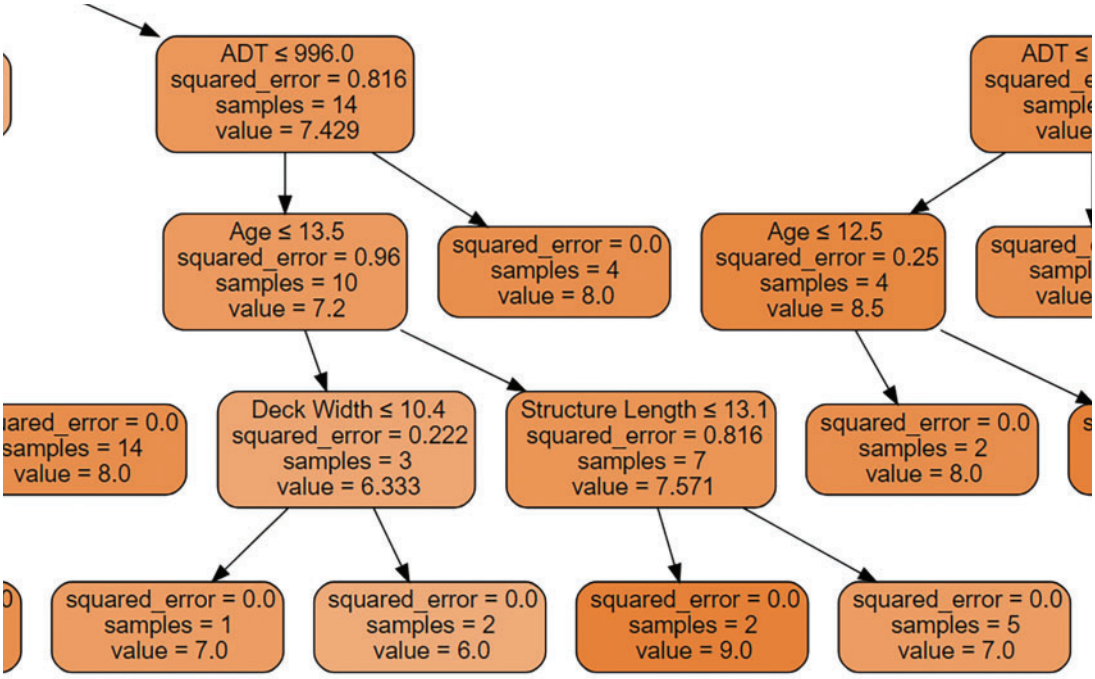

Figure 8. A partial representation of the decision tree model for 1992–2022 concrete bridge data

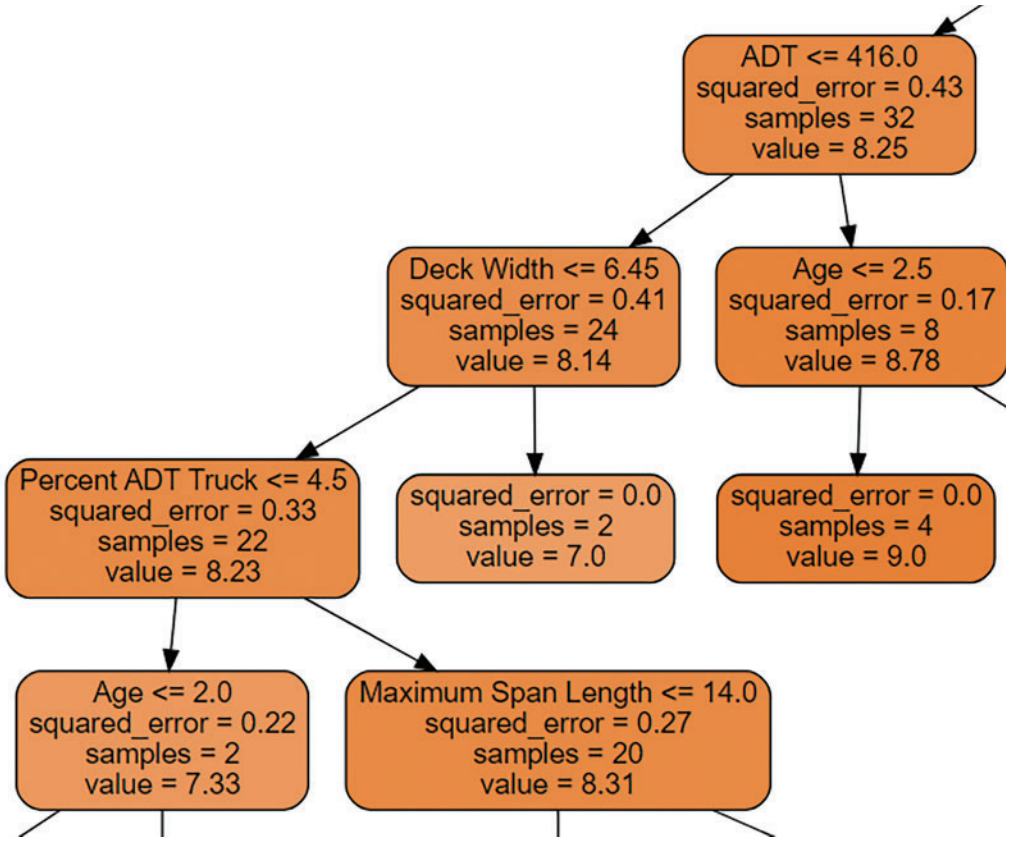

Figure 9. A partial representation of the RF model for 2018–2022 concrete bridge data

materials and model types, while the five-year datasets showed only slight reductions; all values remained above 0.70. The larger dataset, which included over 740,000 bridge records, benefited from repeated observations of the same bridges over time, capturing changes in condition, rehabilitation activities, and characteristics, such as ADT. Although some records were excluded during preprocessing due to incomplete data, the longitudinal nature of the dataset likely improved model performance.

In all cases, the RF model outperformed the DT model. By averaging the outputs of 100 randomized DTs, RF models reduce variance and noise, resulting in more robust predictions. Overall, the RF models trained on the 1992–2022 Concrete Bridge and Steel Bridge datasets achieved the strongest performance. As additional inspection data become available, model accuracy may further improve through continued integration of historical and future records.

Figs. 8 and 9 present sample outputs from the DT and RF models of the Concrete Bridge datasets. Three node types are shown: root, internal, and leaf nodes. The root node is the starting point of the tree from which all branches originate. Internal nodes split into additional nodes based on decision criteria, forming the structure of the tree. Leaf nodes are the terminal nodes and represent the final prediction outcomes, with no further branching.

The DT models can be followed by tracing the characteristic thresholds used at each split. Because most variables in this analysis are quantitative, nodes divide the data using conditions based on values greater than or less than a specified threshold. If the characteristics of a bridge are known, its predicted SER can be determined by following the appropriate path to a leaf node.

Each node contains four key pieces of information. The first row identifies the characteristic and threshold used for the split. The second row shows the squared error, with values closer to zero indicating a more accurate fit. The third row reports the number of bridge samples within the node. This sample size decreases with each split until a leaf node is reached. The fourth row provides the average SER of the bridges contained within that node.

The full DT and RF models generated in this study are too large to display effectively on a single page. To improve interpretability and reduce overfitting, tree size can be controlled through pruning, which removes or prevents splits that do not meet specified criteria, such as a minimum sample size. Tree depth may also be limited. Depth refers to the number of levels between the root and leaf nodes. While deeper trees can improve classification accuracy by capturing more detailed patterns, they also increase the risk of overfitting. Effective model development, therefore, requires balancing predictive performance and generalization.

Both DT and RF models identify patterns in bridge characteristics that predict SER. Each branch represents a sequence of conditions leading to a predicted SER value. For example, in Fig. 8, the root node first splits bridges according to ADT. Subsequent nodes continue to divide the data until groups of bridges with highly similar characteristics remain. The resulting leaf node provides the predicted SER based on the average value of the bridges within that subset. Although RF models consistently outperformed DT models, both demonstrated strong potential as decision-support tools for bridge management.

Because RF visualizations are particularly large, representative paths for concrete bridge and steel bridge models are summarized in Tables 11 and 12, respectively. In the 2022 Concrete Bridge Data model, a sample path begins with a split at bridge age $\leq$31.5 years, containing 6,896 bridges with a squared error of 1.64 and an average SER of 6.94. Moving down the branch by to the left, or the "True" option, the next node was a decision between an age less than to equal to 12.5 years. Here, 3,270 samples were included with a squared error of 1.04 and an average SER of 7.64. Following subsequent age-based splits eventually leads to a leaf node containing five bridges with identical characteristic paths. This node has a squared error of 0.0 and an average SER of 8. Along the path, squared error decreases as additional information is incorporated, indicating improved predictive certainty, while the sample size declines as bridges are partitioned into increasingly specific groups.

The selected path in the 2022 Steel Bridge Data RF model began with a split on deck width $\leq$7.25 m, containing 5,264 bridges with a squared error of 1.81 and an average SER of 6.42. Following the branch for deck widths greater than 7.25 m led to an age-based split, where 4,247 bridges with ages $\leq$19.5 years remained. This node had a squared error of 1.42 and an average SER of 6.68. After ten successive decisions, the path reached a leaf node containing a single bridge with a predicted SER of 8.0.

Table 11. Random forest branch sample information for 2022 concrete bridge data

Characteristic boundary	Boundary decision	Squared error	Sample	Value
Age $\leq$31.5		1.64	6,896	6.94
Age $\leq$12.5	True	1.04	3,270	7.64
Age $\leq$21.5	False	0.92	2,325	7.34
Deck width $\leq$9.05	False	0.97	1,325	7.19
Structure length $\leq$11.5	True	0.91	632	7.36
Deck width $\leq$6.3	True	1.18	226	7.13
Age $\leq$25.5	True	0.76	20	7.67
ADT $\leq$272.0	False	0.43	9	8.20
Structure length $\leq$7.9	True	0.16	7	7.80
ADT $\leq$26.5	False	0.1	6	7.89
	False	0.0	5	8.00

Table 12. Random forest branch sample information for 2022 steel bridge data

Characteristic boundary	Boundary decision	Squared error	Sample	Value
Deck width ≤7.25		1.81	5,264	6.42
Age ≤19.5	False	1.42	4,247	6.68
Age ≤8.5	True	0.74	405	8.04
Structure length ≤199.2	True	0.47	149	8.53
ADT ≤880.0	True	0.42	145	8.56
Deck width ≤10.0	False	0.49	90	8.42
Percent ADT truck ≤6.0	True	1.01	12	7.79
Main unit spans ≤2.0	True	0.96	5	7.2
Percent ADT truck ≤1.5	True	0.4	3	8.0
ADT ≤4080.5	False	0.19	2	7.75
	False	0.0	1	8.0

Similar to the concrete bridge example, the squared error generally decreased as the path progressed toward the leaf node, indicating improved prediction accuracy as additional information became available. Although some nodes exhibited higher squared errors, these deviations may be attributable to limited data for less common characteristics, such as percent ADT truck. The sample size consistently decreased at each split until a single bridge with a unique combination of characteristics remained. Unlike the concrete bridge example, the average SER did not exhibit a consistent trend along this path.

A key advantage of DT and RF models is their ability to clearly visualize how bridges are distributed across characteristic subsets. The paths presented in Tables 11 and 12 represent only two examples from many possible combinations. Every bridge in the dataset is represented within the trees, allowing engineers to explore how specific design or operational characteristics influence predicted SER values. For example, during bridge design, engineers can evaluate how choices, such as the number of main unit spans, may affect the predicted SER.

These models also facilitate the identification of decision points where substantial changes in average SER occur, providing valuable information for inspection planning. Unlike ODOT's AssetWise system, which primarily uses conditional statements based on individual characteristics, RF models evaluate multiple characteristics simultaneously. This capability enables the identification of bridge groups with similar deterioration risks and SER predictions, potentially supporting more targeted inspection intervals.

Effective bridge management depends on both comprehensive documentation and informed decision-making. The proposed models provide engineers with accessible, data-driven insights to support maintenance and rehabilitation decisions. They can function either as standalone screening tools or as enhancements to existing bridge management practices.

Conclusion

This study utilized NBI data for Ohio bridges collected between 1992 and 2022 to develop statistical and supervised machine learning models for predicting the SER. Raw NBI data were imported into Microsoft Excel, where records were organized, cleaned, and filtered. Bridges with incomplete inspection records or inapplicable information were removed. Eight physical and geometric bridge characteristics were selected for analysis, while other variables were excluded and may be investigated in further studies. The remaining data were separated by bridge material into concrete, steel, combined concrete and steel, and other bridge categories. Due to their larger sample sizes, only the Concrete Bridge and Steel Bridge datasets were analyzed, resulting in more than 700,000 usable records. Separate datasets were then created representing the full 31-year period, the most recent five years, and the most recent year.

Data processing and model development were performed using Jupyter Notebook. Three analytical approaches were evaluated: PC, DT, and RF models. PCs quantified the relationships between individual bridge characteristics and SER across the 31-year dataset. Bridge age consistently demonstrated the strongest relationship with SER for both concrete and steel bridges, whereas most other characteristics exhibited weak or negligible correlations. Several results differed from expected trends, and although varying the analysis timeframe affected model performance slightly, it had little influence on the observed correlations.

DT and RF models provided both visual representations of characteristic interactions and accurate SER predictions. The strongest predictive performance was achieved using the complete 31-year datasets, emphasizing the value of comprehensive historical inspection records. Among the machine learning approaches, RF models consistently outperformed DT models while maintaining strong interpretability.

The findings demonstrate the usefulness of all three methods for supporting bridge management decisions. PCs help identify characteristics most closely associated with bridge

condition, while DT and RF models reveal how combinations of characteristics influence SER. These tools could support future bridge inspection programs by identifying bridges that warrant increased monitoring. Unlike traditional screening methods that rely on individual criteria, machine learning models can evaluate multiple characteristics simultaneously, improving the precision of bridge selection. Integrating these models with existing systems, such as AssetWise, could help prioritize the most critical bridges within already-flagged populations. As bridge infrastructure continues to age, data-driven tools can enhance inspection planning, maintenance prioritization, and rehabilitation strategies, ultimately improving public safety and the long-term management of transportation assets.

Data Availability Statement

All data related to this research are available upon request.

References

[1] Federal Highway Administration (FHWA). *Bridge Replacement Unit Costs 2022*. Washington DC, USA: Bridges and Structures; 2022. https://www.fhwa.dot.gov/bridge/nbi/sd2022.cfm#c.

[2] Hartmann J, Weingroff R. *Highway History*. Washington DC, USA: Federal Highway Administration; June 2021. https://www.fhwa.dot.gov/highwayhistory/national_bridge_inspection_standards.cfm#:~:text=The%20modern%20highway%20bridge%20safety,and%20unsafe%20bridges%20are%20.

[3] Gee K, Henderson G. *Highway Bridge Inspections*. Washington DC, USA: U.S. Department of Transportation; 2007. https://www.transportation.gov/testimony/highway-bridge-inspections.

[4] Ohio Department of Transportation (ODOT) Office of Structural Engineering. Columbus, Ohio, USA: Reliability Based Inspection (RBI) Implementation Procedure; 2021. https://www.transportation.ohio.gov/business/engineering/structural.

[5] Federal Highway Administration (FHWA). Nondestructive evaluation and structural health monitoring. In: *Nondestructive Evaluation and Structural Health Monitoring*. FHWA; 2021. https://highways.dot.gov/research/long-term-infrastructure-erformance/ltbp/nondestructive-evaluation-structural-health-monitoring#tools.

[6] National Highway Traffic Safety Administration (NHTSA). *Traffic Safety Facts 2021: A Compilation of Motor Vehicle*. Washington DC, USA: Federal Highway Administration; 2023. https://crashstats.nhtsa.dot.gov/Api/Public/ViewPublication/813527.

[7] Palu S, Mahmoud H. Impact of climate change on the integrity of the superstructure of deteriorated U.S. bridges. *PLoS One*. 2019;14(10). doi:10.1371/journal.pone.0223307.

[8] Zhao R, Shi C, Zhang R, Wang W, Zhu H, Luo J. Study on the freeze-thaw resistance of concrete pavements in seasonally frozen regions. *Materials*. 2024;17(8):1902. doi:10.3390/ma17081902.

[9] Clarke-Sather AR, McConnell JR, Masoud E. Application of lean engineering to bridge inspection. *J Bridge Eng*. 2021;26(2). doi:10.1061/(asce)be.1943-5592.0001657.

[10] Abdallah AM, Atadero RA, Ozbek ME. A state-of-the-art review of bridge inspection planning: current situation and future needs. *J Bridge Eng*. 2022;27(2). doi:10.1061/(asce)be.1943-5592.0001812.

[11] Galdelli A, D'Imperio M, Marchello G, Mancini A, Scaccia M, Sasso M, Frontoni E, Cannella F. A novel remote visual inspection system for bridge predictive maintenance. *Remote Sens*. 2022;14(9):2248. doi:10.3390/rs14092248.

[12] Duque L, Seo J, Wacker J. Bridge deterioration quantification protocol using UAV. *J Bridge Eng*. 2018;23(10). doi:10.1061/(asce)be.1943-5592.0001289.

[13] Altmann ML, Benthien T, Ellendt N, Toenjes A. Defect classification for additive manufacturing with machine learning. *Materials*. 2023;16(18):6242. doi:10.3390/ma16186242.

[14] Patro KK, Jaya Prakash A, Jayamanmadha Rao M, Rajesh Kumar P. An efficient optimized feature selection with machine learning approach for ECG biometric recognition. *IETE J Res*. 2020;68(4):2743–2754. doi:10.1080/03772063.2020.1725663.

[15] Armin RN, Hazem E. Predicting Ohio bridges' conditions using multi-target machine learning algorithms. *Proceedings of the International Conference on Transportation and Development 2024*. Reston, VA: American Society of Civil Engineers; 2024. doi:10.1061/9780784485538.055.

[16] Luo K, Kong X, Zhang J, Hu J, Li J, Tang H. Computer vision-based bridge inspection and monitoring: a review. *Sensors*. 2023;23(18):7863. doi:10.3390/s23187863.

[17] Li Z, Burgueño R. Using soft computing to analyze inspection results for bridge evaluation and management. *J Bridge Eng*. 2010;15(4):430–438. doi:10.1061/(asce)be.1943-5592.0000072.

[18] Federal Highway Administration (FHWA). *Recording and Coding Guide of the Structure Inventory and Appraisal of the Nation's Bridges*. Washington DC, USA; 1995. https://www.fhwa.dot.gov/bridge/mtguide.pdf.

[19] Phares BM, Washer GA, Rolander DD, Graybeal BA, Moore M. Routine highway bridge inspection condition documentation accuracy and reliability. *J Bridge Eng*. 2004;9(4):403–413. doi:10.1061/(asce)1084-0702(2004)9:.

[20] LeBeau K, Wadia-Fascetti S. Predictive and diagnostic load rating model of a prestressed concrete bridge. *J Bridge Eng*. 2010;15(4):399–407. doi:10.1061/(asce)be.1943-5592.0000073.

[21] Agrawal AK, Kawaguchi A, Chen Z. Deterioration rates of typical bridge elements in New York. *J Bridge Eng*. 2010;15(4):419–429. doi:10.1061/(asce)be.1943-5592.0000123.

[22] Tabatabai H, Tabatabai M, Lee C-W. Reliability of bridge decks in Wisconsin. *J Bridge Eng*. 2011; 16(1):53–62. doi:10.1061/(asce)be.1943-5592.0000133.

[23] Saberi MR, Rahai AR, Sanayei M, Vogel RM. Bridge fatigue service-life estimation using operational strain measurements. *J Bridge Eng*. 2016;21(5). doi:10.1061/(asce)be.1943-5592.0000860.